

Whirl Orbital Response Control of Micro Rotors With Flexural Modes

Abhro Mukherjee and Satyabrata Das

National Institute of Science and Technology, Odisha, India.

Sabyasachi Sengupta

Indian Institute of Technology, Kharagpur, India.

(Received 16 December 2015; accepted 13 September 2016)

In this paper there is an attempt to develop an elegant controlling strategy to stabilize flexible rotors having flexural modes. Initially, the possible causes of instability in a rotor system due to internal damping through mathematical formulation are discussed. The threshold or the critical speed was derived beyond which the rotor became unstable. The stabilizing algorithm was designed by keeping the overall control law mathematically simple such that minimum numbers of sensors were used and deployed. Actuators were properly selected such that control and stabilization was practically possible for rotors of such low diameters. Bond graphs were used to model the rotor system having flexural modes. As bond graphs act as a portrayal of power and information exchange within the system and with external environment, bond graphs may give a better clue for modeling such systems. The real challenge in this work lies in the proposal of control strategy in stabilizing non-rigid rotors having flexible modes. Mathematical simplicity of the proposed control algorithms is considered for its easy deployment. The Simplest Beam model the Euler-Bernoulli beam is considered.

NOMENCLATURE

R_a	Stationary damping of the shaft
R_i	Shaft rotating damping
V_f	Velocity at fixed reference frame
V_r	Velocity at rotating frame
K_s	Stiffness of the rotor
F_c	Circulating force
w	Running speed of the rotor
m	mass of the rotor
A	Orbital area of the shaft
L	Length of the shaft
R_{eq}	Effective value of the rotating damper
R_c	Negative damping coefficient
w_n	Natural frequency shaft
$(\mu_{XX}, \mu_{XY}, \mu_{YY}, \mu_{YX})$	The modulus of various transformers
V_{amp}	Whirl orbital response function
ε	Eccentricity of the shaft
η	Switching Function
R_{ieff}	Effective internal or rotating damping
F_{orbes}	Whirl orbital function
Φ	Potential function
ρ	Density of the beam
E_l	Flexural rigidity
(w_i, w_j)	i th and j th mode of frequency
$y(x, t)$	Vertical displacement beam

1. INTRODUCTION

Destabilizing effect is very common phenomena in rotating or gyrating systems. Rotors at speeds higher than certain threshold values become unstable due to rotating damping forces generated by dissipation in rotor material. The causes of instability of rotor systems due to internal damping was addressed by several authors.^{1-5, 10-12} Interestingly, several attempts were made earlier to stabilize such systems. Authors have shown that how anti-symmetric transformation matrices were responsible for creating these instabilities. Although the current methods in practice are quite effective for large- or medium-size rotors, these may not be suitable for small-, mini-, or micro-size rotor systems. There have been considerable efforts in the past to stabilize rotors with large diameters using conventional control algorithms like sliding mode or adaptive control techniques, but due to complexity in the control algorithm or lack of information on the type of disturbance model, the overall design has become too complicated for real time implementation of such systems. Some papers based on conventional control methods to stabilize rotors essentially with large diameters with flexible modes are worth mentioning.¹³⁻²⁶ This paper benefits from handling the control law equation with minimum complexity such that deployment of control law in real time would be simple. The real challenge in this work lies in the proposal of a stabilizing strategy that could arrest instability caused due to modal spillover. One may consider an Euler- Bernoulli beam model and then orthogonal separation of various modal components of a uniform beam can be done. Thereafter, each flexural mode was modeled by using Bond graphs and finally integrated into a single model. For modeling

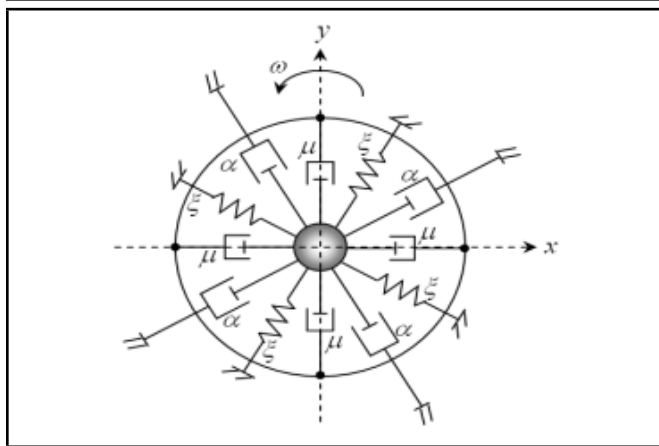


Figure 1. Schematic Representation of rotor shaft with fixed and rotational dampers.

the system of flexible rotors with different modal components, the following papers²⁷⁻³¹ were referenced to build the complete model. Initially, the system was kept uncontrolled without any controller and instability was clearly visible through simulated results. Later, the controller was implemented within the bond graph model and the stabilizing effects of the controlling strategy were shown through simulation. The control strategy used here is the whirl orbital response type controller. The overall mathematical structure of the controller is shown in the sections below and efficacy of the controller is validated through simulation results. The controller is attached within the bond graph and no additional design using any other control system design toolbox is used in the model.

2. ANALYSIS OF ROTORS WITH INTERNAL DAMPING

The aerial damping coefficient is taken as $\alpha = R_a/2$, such that effective damping coefficient in all direction is R_a . Here the frame is taken as $\mu = R_i/2$, such that its effective value in all directions is R_i . Both R_a and R_i are stationary and rotating damping, respectively. The stiffness is assumed to be $\xi = K_s/2$, such that stiffness K_s is experienced in all directions. For general dynamics and nature of the non-potential force, one may refer to.^{32,33} The internal damping forces act along with the rotating frame. The velocity in the rotating frame is related to those in fixed frame in co-oriented and coordinate as follows (i, j, k are the unit vectors). The equation below can be written from the geometrical constraint between fixed and rotating frames. The dynamics are captured in a situation where the frames are co-oriented but non co-rotating:

$$V_f = V_r + \omega \times r = V_r + \omega \hat{k} \times (\hat{x}_i + \hat{y}_j) = V_r + \omega \hat{y}_i - \omega \hat{x}_j. \quad (1)$$

In matrix notations:

$$\begin{bmatrix} V_{x,f} \\ V_{y,f} \end{bmatrix} = \begin{bmatrix} V_{x,r} \\ V_{y,r} \end{bmatrix} + \begin{bmatrix} 0 & \omega \\ -\omega & 0 \end{bmatrix} \begin{bmatrix} X \\ Y \end{bmatrix}. \quad (2)$$

In terms of displacement components:

$$\begin{bmatrix} \hat{X}_r \\ \hat{Y}_r \end{bmatrix} = \begin{bmatrix} \hat{X}_f \\ \hat{Y}_f \end{bmatrix} + \begin{bmatrix} 0 & -\omega \\ \omega & 0 \end{bmatrix} \begin{bmatrix} X \\ Y \end{bmatrix}. \quad (3)$$

The damper force vector would be obtained by multiplying with R_i :

$$\begin{bmatrix} F_x \\ F_y \end{bmatrix} = R_i \begin{bmatrix} \hat{X}_f \\ \hat{Y}_f \end{bmatrix} + \begin{bmatrix} 0 & -\omega R_i \\ \omega R_i & 0 \end{bmatrix} \begin{bmatrix} X_f \\ Y_f \end{bmatrix}. \quad (4)$$

The second term of the above equation is circulating force and it is non-potential in nature, which means mathematically the curl taken of this force would remain non-zero. Hence, the work done by circulating force F_C will be path-dependent. If a point is moved in a circular orbit around its equilibrium point at $X = Y = 0$ then work done in such an orbit will be:

$$W_c = \oint \bar{F}_c \cdot d\bar{r} = \iint (\nabla \times \bar{F}_c) \cdot d\bar{a} = \iint 2\omega R_i \hat{k} \cdot d\hat{a} = 2\omega R_i A. \quad (5)$$

The area A is positive if the rotor center orbits in the same direction (clockwise or counter-clockwise) as the spin angular velocity of the rotor, otherwise area A will be negative.

3. FLEXIBLE ROTOR WITH SMART COUPLING AND DRIVE

The rotor system shown in Fig. 2 has all the essential features which are to be addressed. It comprises free-to-oscillate rotors. In the two orthogonal planes, the external dampers are attached. Isotropic stiffness and internal damping in the rotor are lumped in the flexible coupling connecting the constant speed drive and the rotor. Within the coupling, the sensing and the actuating elements are embedded. The sensing and actuating elements may be practically realized by deployment of a set of piezo-actuators. As all dynamics are captured in the rotating frame, to model the system systematically, frame transformation from fixed to rotating frame is considered.

4. THRESHOLD SPINNING SPEED AND STABILIZING STRATEGY

One of the important things is to find out the critical speed of the rotor. A simple way of doing this is to convert the bond graph into a signal flow graph and then, using the characteristics equation threshold, speed can be found out. Alternatively, we can always equate the dissipative power and regenerative power to find out the critical speed of the rotor beyond which the system would be unstable. Once it becomes unstable, the power drawn from the shaft increases monotonically. Here the threshold speed depends on the shaft natural frequency $\sqrt{K_S/m}$ and external damping R_a and material or rotating damping R_i . At speeds $\omega > \omega_{th}$ the regenerative energy per orbit or regenerative power will be larger than power dissipated by damping $R_a + R_i$. The system will become unstable and there will be continuous growth of the power drawn from the shaft. This can be observed by the simulated result in the later part of the paper. It has been observed from Eq. (7) that the critical spinning speed depends on the shaft natural frequency $\sqrt{\frac{K}{m}}$, the external damping R_a and also rotating damping R_i .

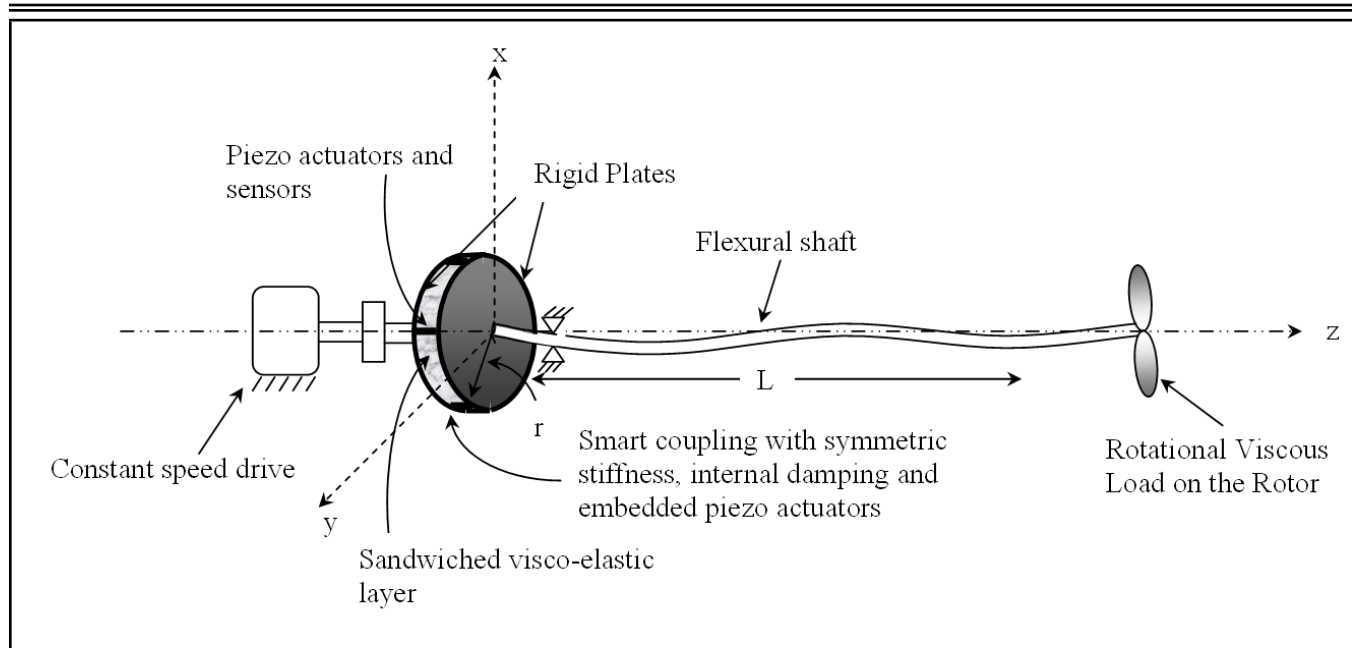


Figure 2. Schematic diagram of the rotor system with flexural mode.

Therefore, it is possible to achieve stability by increasing the value of ω_{th} (refer to the relation $\omega_{th} = \omega_n(1 + R_a/R_i)$) beyond the running speed ' ω '. We may modulate directly the shaft stiffness parameter ' K ' as the stiffness coefficient is dependent on the threshold speed ω_{th} here. This way of stabilization would be impractical as it may pose tremendous challenges for modulating the stiffness of the rotor of a rotating shaft with minimum number of actuators. Papers^{32,33} may be referred to for in-depth derivation of the critical threshold speed of the rotor. Increasing the shaft stationary damping R_a is another way by which we could shift the shaft critical speed. Refer to papers²⁷ where the authors have used squeeze film dampers to enhance stability; however, these methods were restricted strictly for large- and medium-size rotors as the size of the squeeze film dampers has limitations as it may not be the right choice to use these sort of dampers for low-diameter rotors. By applying velocity proportional force in stationary frame on the shaft, one may artificially increase R_a . This will lead to an increase in ω_{th} . However, depending on the range $\omega - \omega_{th}$, the difference of spinning, and the instability onset speed, the feedback gains will have to be increased. For larger differences of these speeds, larger gain would be needed. This would certainly mean a larger actuation problem and hence large size actuators are actually required which may not be feasible to stabilize rotors of certain descriptions and size. In addition to this for application of these forces, a rigid stationary structure would be needed which may not be practically implemented, especially with rotors with such a low diameters. There would be severe constraints and problems to integrate such systems with the rotating shaft and this will surely affect ones primary goal to stabilize rotors of mini or micro size. There may also be additional problems arising in implementing such systems due to high contact friction and wear in the actuators. If one recalls the relation of the instability threshold speed $\omega_{th} = \omega_n(1 + R_a/R_i)$. The term R_i appears

in the denominator which determines the internal damping in rotating frame. Now if by control action, that is by applying forces proportional to the velocities in rotating frame, the effective internal damping may be modulated. This will lead to high values of ω_{th} . One may say $R_{eqv} = R_i - R_c$, where R_{eqv} is the effective value of rotating damping. R_{eqv} is the original material damping and R_c is the negative damping created by the control action. With this control the effective ω_{th} would be:

$$\omega_{th} = \omega_n(1 + R_a/(R_i - R_c)) = \omega_n(1 + R_a/R_{eqv}). \quad (6)$$

This control has several advantages. This has to be implemented in a frame rotating with the shaft or on the shaft itself. Thus, using this method one may use smart structures effectively. Piezo actuators (PZT's), electromagnetic devices in rotating frames, may be used for relatively larger rotors. As the limit of R_c is from 0 to R_i then for whole range of spinning speeds, the gain values and controller actuation forces are also limited and it does not reach very high unacceptable values and may be achieved at modest feedback gains.

It has been shown in the simulation results later that the shaft-drawn power monotonically increases when the shaft becomes unstable. Thus in design of R_c the shaft-drawn power from the drive may be used. The most significant requirement is that once the shaft attains stability and the shaft-drawn power comes to zero, this terminal R_c value should get latched. The proposed design of R_c is as follows:

$$R_c = \alpha P + \int_0^t P(\varepsilon) d\varepsilon + \sigma \frac{dP}{dt}. \quad (7)$$

Here α , β , and σ are controller tuning parameters and $P(\varepsilon)$ is the shaft-drawn power, which is the amount of power the shaft draws from the source which renders it unstable.

If we recall for the threshold speed $\omega_{th} = \omega_n(1 + R_a/R_i)$. the control action keeps increasing this threshold speed by re-

ducing the effective rotating damping. The following equations will give more detailed explanation of the dynamics:

$$\omega_{th} = \omega_n(1 + R_a/(R_i - \alpha P - \beta \int_0^t P d\xi - \sigma dP/dt)). \quad (8)$$

Once ω goes past the running speed, the shaft is stabilized ex when $\omega_{th} \geq \omega$.

4.1. Stabilization Algorithm with Whirl Orbital Response Control

The previous section suggests that the design parameter R_c should be determined by some response function which is related to power going for whirling motion only and which by any means should not be the power going to the load. The control algorithm of equation (8) has a limitation that we cannot absolutely determine the amount of power which renders the shaft unstable as a certain amount of power is utilized by the load. Therefore, we need further modification on the control algorithm. Instead of directly measuring the shaft-drawn power, one could take a response function proportional to the orbital radius in rotating frame or it could be a better and even superior response function if we take it as $\dot{x}_r^2 + \dot{y}_r^2$. The main idea here is to create a response function whose determination would give the actual power drawn by the shaft that renders the shaft unstable. Determination of a response function based on velocity would be easily measured as compared to sensing actual shaft-drawn power which creates the whirling motion of the shaft. The modified control algorithm thus looks like:

$$R'_c = (\alpha * V^2_{amp} + \beta * \int_0^t V^2_{amp} dt + \sigma * dV^2_{amp}/dt); \quad (9)$$

$$V^2_{amp} = \left(\hat{X}_r * \frac{r}{L} \right)^2 + \left(\hat{Y}_r * \frac{r}{L} \right)^2. \quad (10)$$

For a perfectly balanced shaft with load, the shaft power drawn is the sum of the power which fosters the whirling motion and the power needed by the load. If R_c becomes larger than the internal damping R_i and as a result R_{eqv} becomes negative leading to the occurrence of eventual reverse whirl which may rapidly grow in amplitude. This can again destabilize the shaft. To prevent this type of reverse whirl occurrence we have improvised the existing control by addition of a switch.

$$F_{orbes} = (\dot{x}_r^2 + \dot{y}_r^2) * \eta. \quad (11)$$

Here a new switching variable η is added to the whirl orbital function F_{orbes} . Therefore the design parameter now can be determined by:

$$R_c = \alpha F_{orbes} + \beta \int_0^t F_{orbes} dt + \gamma dF_{orbes}/dt. \quad (12)$$

The effective internal or rotating damping $R_{ieff} = R_i - R_c$. Now switching conditions may be If $R_c < R_i$ then $\eta = 1$. If

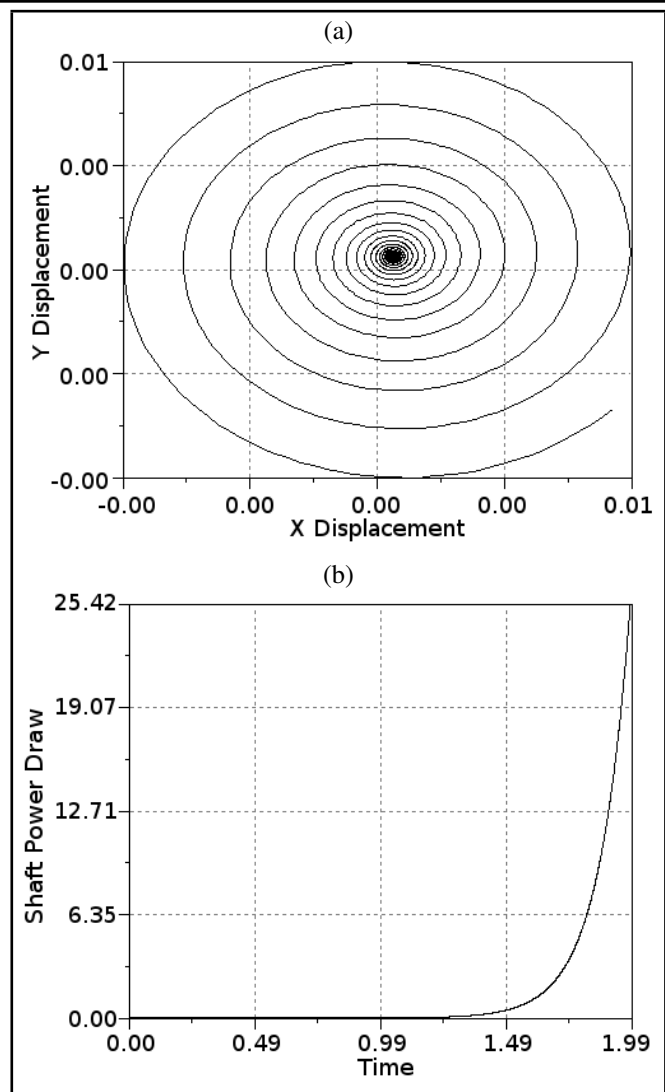


Figure 3. (a) Instability in XY plane. (b) Shaft drawn power without the controller.

$R_c > R_i$ then $\eta = -1$. If $R_c < R_{ieff}$ then the switching function $\eta = 1$ which implies that the controller operates normally. If $R_c > R_{ieff}$ then the switching function $\eta = -1$ which means that the controller has to make sure that the rotor does not undergo a reverse whirl. For the condition $R_c = R_{ieff}$, to avoid redundancy, we need to take the value of $\eta = 0$.

5. DYNAMICS OF ROTOR WITHOUT STABILIZING STRATEGY

The rotor is rotated at a speed beyond ω_{th} . There is no eccentricity. The rotor was given an initial momentum in x -direction. The bond graph model shown in Fig. 4 is a very good tool for creating mathematical models of complex systems having interplay of several energy domains in a unified manner. The plot in Fig. 3a shows that orbit keeps on increasing with time and Fig. 3b shows that the shaft power drawn increases monotonically at a very fast rate.

5.1. Stabilization of Rigid Rotor Using Whirl Orbital Response

For stabilization of the rotor, the design parameter R_C should be determined by some response function which is related to power going for whirling motion only and which is not at all related to power which is rendered to the shaft load. The orbital area is one such response function. However, an even better response function would be $\dot{X}_r^2 + \dot{Y}_r^2$. In the following simulations this function is implemented by taking,

$$R'_c = \alpha * V_{amp}^2 + \beta * \int_0^t V_{amp}^2 dt + \sigma * \frac{dV_{amp}^2}{dt}. \quad (13)$$

The Figs. 5a and 5b shows the vibration amplitudes in fixed and rotating frames for balance shaft with a relatively large shaft load. This strategy stabilizes the rotor even with such shaft loads as expected. The stabilizing action of the controller is completely visible from Fig. 5c. Initially the shaft-drawn power increases until a peak and thereafter decreases monotonically and the excess power drawn is returned back to the system, thus stabilizing the shaft.

Figures 6a and 6b is the response shown of the same shaft with eccentricity of 1.0×10^{-4} with this proposed stabilizing strategy. This is an extremely satisfactory dynamic behavior of the rotor.

An alternative orbit response function could be the sum of absolute values of orthogonal velocity components in rotation frame as follows.

$$R'_c = (\alpha * V_{abs} + \beta * \int_0^t V_{abs} dt + \sigma * dV_{abs}/dt); \quad (14)$$

$$V_{abs} = \left| \left(\dot{X}_r * \frac{r}{L} \right) \right| + \left| \left(\dot{Y}_r * \frac{r}{L} \right) \right|. \quad (15)$$

The below response shows the vibration amplitudes in fixed and rotating frames for a balanced shaft with a relatively large shaft load, $R_l = 0.001$ Nms. The power drawn by the shaft fluctuates about the load and then settles at this value once the whirl is stabilized.

Though initially the theory of stabilization was built on the basis of power drawn by the shaft, for other considerations like shaft load and eccentricities, one of the orbital response functions, like square of velocity amplitude or sum of absolute values of orthogonal components of velocities in a frame rotating with the rotor, should be a favored function. The square of the velocity amplitude is proportional to that part of shaft-drawn power which fosters whirling of the shaft, whereas the absolute velocity sum is a function which increases with area and thus we can actually get the power drawn by the shaft to create the whirling motion. In fact, in adapting one of these strategies, one has not departed from the original proposal but modified it for a broader set of operating conditions.

6. ORTHOGONAL SEPARATION OF VARIOUS MODAL COMPONENTS OF A UNIFORM EULER BERNOULLI BEAM TYPE ROTOR

The Euler Bernoulli beam equation is given by:

$$\rho A \ddot{Y}(x, t) + EI \partial^4 Y(x, t) / \partial x^4 = 0. \quad (16)$$

Let the solution of this differential equation be given as $y = Y(x) \cos(\omega t)$, here $Y(x)$ is given by natural motion of the beam.

The beam model now can be written as:

$$(-\rho \omega^2 Y(x) + EI d^4 Y(x) / dx^4) \cos(\omega t) = 0; \quad (17)$$

$$k^4 = A \rho \omega^2 / EI; \quad (18)$$

$$k = (A \rho \omega^2 / EI)^{1/4}; \quad (19)$$

$$Y(x) = 1/k^4 (d^4 Y(x) / dx^4); \quad (20)$$

$$Y(x) = A \cos(kx) + B \sin(kx) + C \cosh(kx) + D \sinh(kx). \quad (21)$$

Boundary Conditions can be used for the following combinations to find out the value of 'k' and the modal frequencies ω : pinned-fixed or fixed-pinned; pinned-free or free-pinned; pinned-guided or guided-pinned; fixed-free or free-fixed; fixed-guided or guided. A pinned-free type of beam structure is considered.

Consider the i th mode:

$$w_i^2 Y_i(x) = \xi d^4 Y_i(x) / dx^4. \quad (22)$$

Consider the j th mode:

$$w_j^2 Y_j(x) = \xi d^4 Y_j(x) / dx^4. \quad (23)$$

Multiplying the first equation by Y_j and the second equation by Y_i we get the following equations for $i \neq j$:

$$w_i^2 Y_i Y_j = \xi Y_j d^4 Y_i(x) / dx^4; \quad (24)$$

$$w_j^2 Y_j Y_i = \xi Y_i d^4 Y_j(x) / dx^4. \quad (25)$$

Integrating the above equations we get:

$$w_i^2 \int_0^t Y_i Y_j . dx = \xi \int_0^t Y_j d^4 Y_i / dx^4 dx; \quad (26)$$

$$w_j^2 \int_0^t Y_i Y_j . dx = \xi \int_0^t Y_i d^4 Y_j / dx^4 dx. \quad (27)$$

Subtracting the above two equations we get:

$$(w_i^2 - w_j^2) \int_0^l Y_i Y_j dx = 0. \quad (28)$$

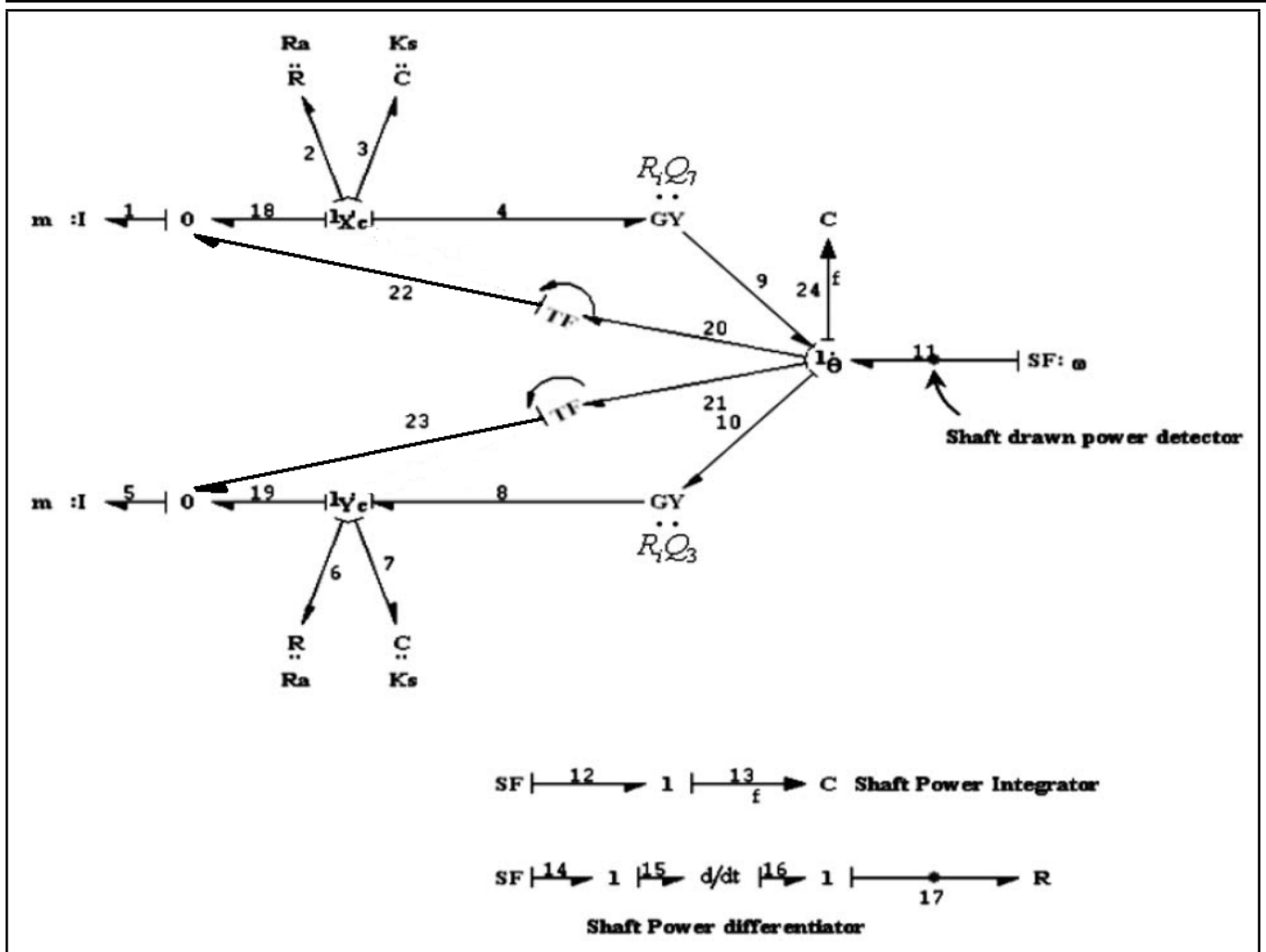


Figure 4. Simple rotor model with stabilizing strategy incorporated.

The orthogonal condition will thus become:

$$\int_0^l Y_i Y_j dx = 0 \quad \text{for } i \neq j. \quad (29)$$

The above property can be used for modal separation of beam frequencies. Further the normalized equation can be given by:

$$\hat{Y}_i = Y_i / \sqrt{\int_0^l Y_i Y_i dx}. \quad (30)$$

$\hat{Y}_i(x)$ are normalized ortho-normal modes which will satisfy:

$$\int_0^l \hat{Y}_i \hat{Y}_i dx = 1 \quad \text{and} \quad \int_0^l \hat{Y}_i \hat{Y}_j dx = 0. \quad (31)$$

$$\hat{Y}_i = (\cosh(q_i * (L - x)) + \cos(q_i * (L - x)) - (\sinh(q_i * (L - x)) + \sin(q_i * (L - x))) / \sqrt{L}; \quad (32)$$

$q_1 * L = 3.966$, $q_2 * L = 7.0686$, $q_3 * L = 10.2102$, $q_4 * L = 13.3518$ and in general for $i > 4$ $q_i = (4 * i + 1) * \pi / 4$.

7. MODELING OF ROTOR SYSTEM WITH FLEXURAL MODES ATTACHED

There may be several ways of modeling dynamical systems. The governing equation for the rotor system with the spinning dampers can be shown below,

$$m \begin{bmatrix} \hat{x} \\ \hat{y} \end{bmatrix} = -K \begin{bmatrix} x \\ y \end{bmatrix} - R_i \begin{bmatrix} \hat{x} \\ \hat{y} \end{bmatrix} + \begin{bmatrix} 0 & \omega R_i \\ -\omega R_i & 0 \end{bmatrix} \begin{bmatrix} x \\ y \end{bmatrix}. \quad (33)$$

This way of writing the model equation is good but it does not reveal from where the circulating force (which is the third term on right side) imports power. The physics behind the dynamics of this system remains obscured. Alternatively, a bond graph model may be created. As bond graphs are portrayals of power and information exchange within the system and with an external environment, bond graphs may give better clues to this issue. The model reveals that the regenerative power of circulating forces comes to the system from the drive through gyration actions as modeled using a pair of gyrators. The regenerative power of circulating forces comes to the system from the drive. The component of the velocity of the mass center of

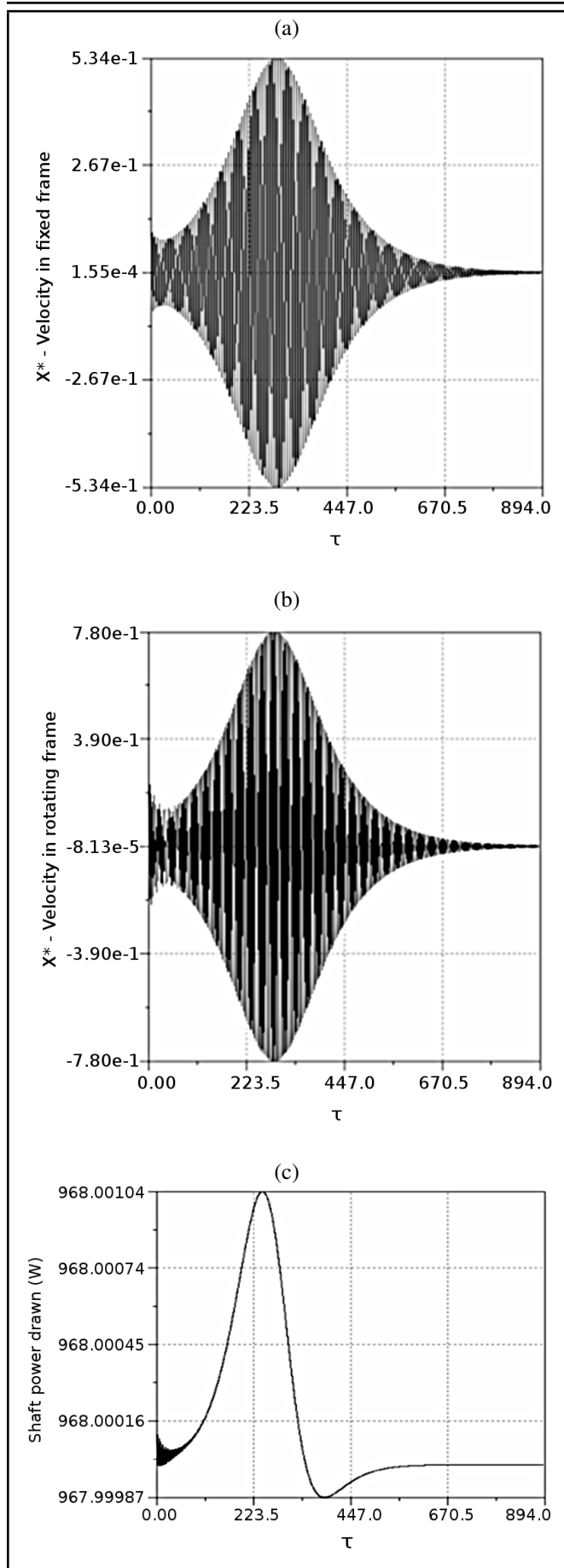


Figure 5. (a) X displacement of the shaft in fixed frame. (b) X displacement in rotating frame. (c) The shaft drawn power.

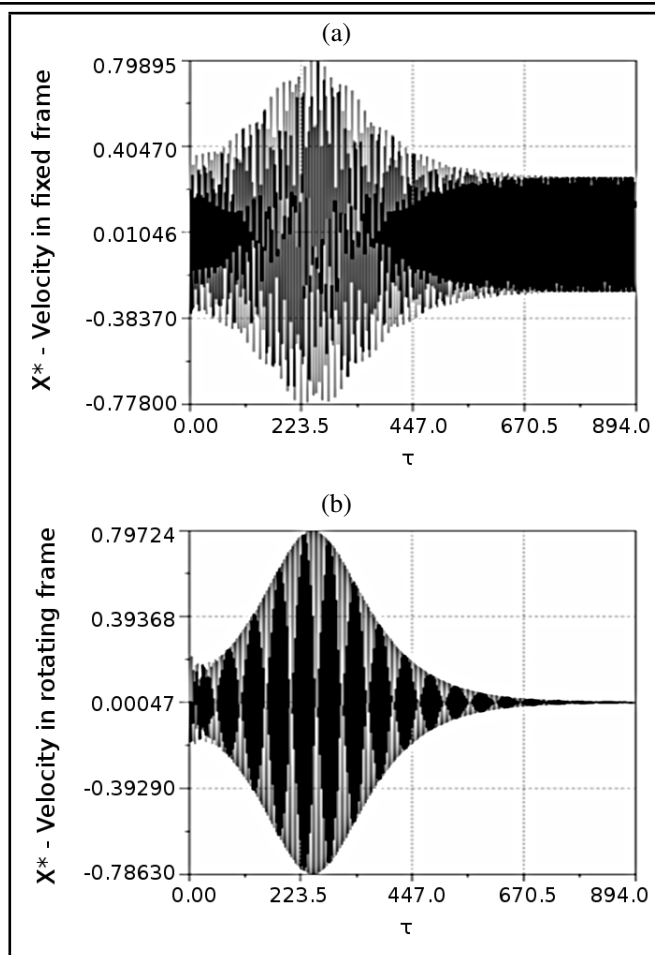


Figure 6. (a) X displacement of the shaft in fixed frame rotating using whirl orbital response. (b) X displacement of the shaft in frame using whirl orbital response.

the disk may be written as follows:

$$\begin{aligned} \dot{x}_m &= \dot{x} - \varepsilon\omega * \sin(\omega t + \varphi); \\ \dot{y}_m &= \dot{y} + \varepsilon\omega * \cos(\omega t + \varphi). \end{aligned} \quad (34)$$

The smart structure (piezo-actuator), which will be providing the actual controlling action, will be rotating along with the rotor structure; therefore, it is important for us to model all dynamics in rotating coordinates. The fundamental equations for the basic transformations are as follows,

$$\dot{X}_p = \cos \theta \dot{X} + \sin \theta \dot{Y} + (-\sin \theta X + \cos \theta Y) \dot{\theta}; \quad (35)$$

$$\dot{Y}_p = -\sin \theta \dot{X} + \cos \theta \dot{Y} + (\cos \theta X + \sin \theta Y) \dot{\theta}. \quad (36)$$

The piezo-actuators are all coupled together in a crystal-like structure. The entire structure rotates along with the shaft; therefore, all dynamics are seen from the rotating frame.

8. BRIEF DISCUSSION ON THE SIMULATION

Two sets of simulation results are shown below. In section 8.1, no active stabilizing controller is used and the tuning parameters are kept at zero value. In section 8.2, the controller is actively used and the rotor attained stabilization, which is shown in the simulation results below.

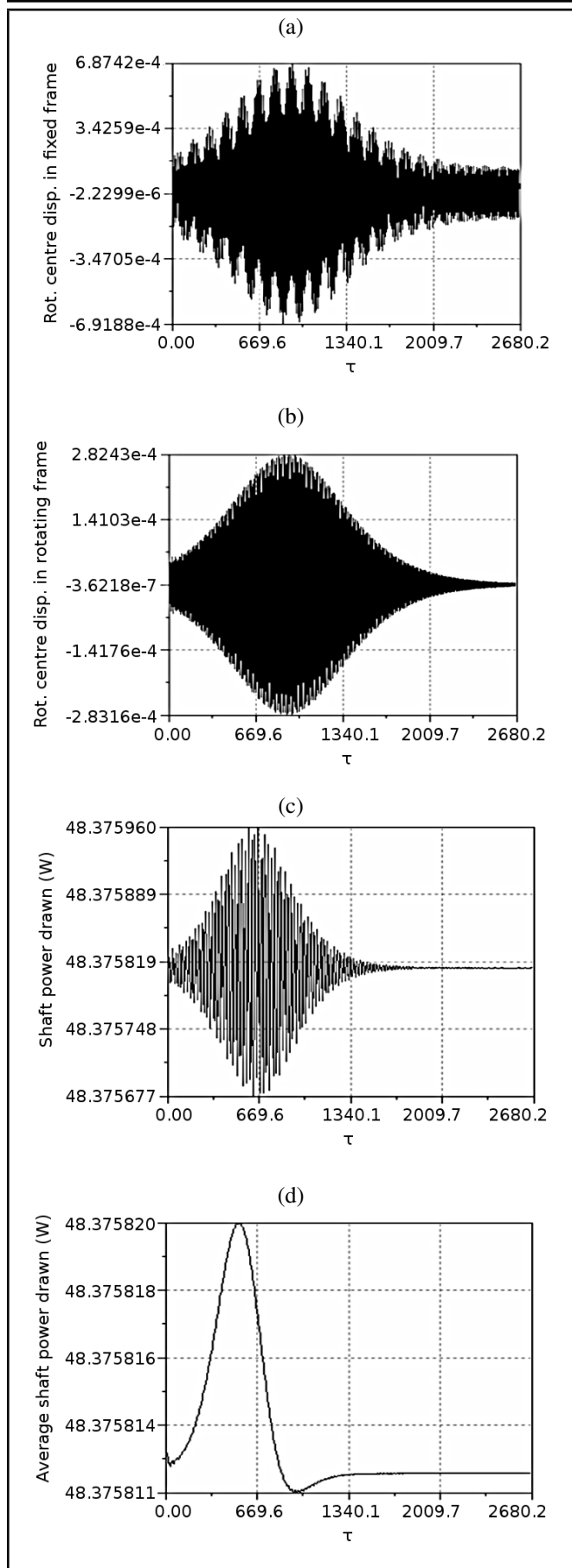


Figure 7. (a) Rotational displacement of the center in fixed frame. (b) Rotational displacement of the center in rotating frame. (c) Shaft drawn power. (d) Average shaft drawn power.

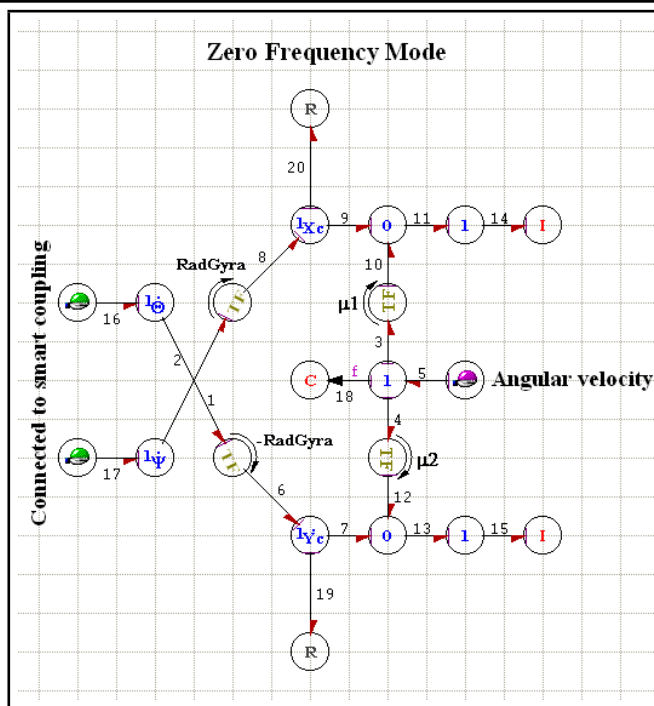


Figure 8. Bond graph model of zero-frequency mode.

8.1. Rotor Response Without Active Stabilization

From Fig. 10a we observed that the simulation result continues to show an unstable spiral-like orbit in rotating frame for zeroth mode of oscillation. Further, Fig. 10b shows that the rotor still exhibits unstable whirl with respect to fixed reference frame. Figure 10c shows the first modal component in static frame and as the controller tuning parameters are kept at zero, the dynamics are virtually uncontrolled and show an unstable whirling motion. Higher modal components – the second and third modal component in static frame – shows whirl-like instability as the controller is not in action and the dynamics are uncontrolled. The above simulated dynamics portray the non-potential nature of the circulating force with non-vanishing curl as discussed in the previous section which drives the shaft to become unstable and the shaft continues to draw power from the constant speed drive.

8.2. Stabilization of the Rotor with Attached Controller

To stabilize the rotor, the active stabilizer is attached with the system. The tuning parameters are given by a finite value.

Though with much smaller gains the system gets stabilized but has a somewhat longer simulation time. The stable responses of the rotor, due to active stabilization, are shown below. From Fig. 11a, the active stabilizing controller is attached with the rotor system and the controller has already stabilized the zeroth mode with its control action. We can also see that the stabilization can be seen from the convergence of whirling motion at a definite value both for X and Y directions. Figure 11c shows the first modal component getting stabilized by the controller action. We have already given some values to the tuning parameters unlike in case 1 where the controller was kept out

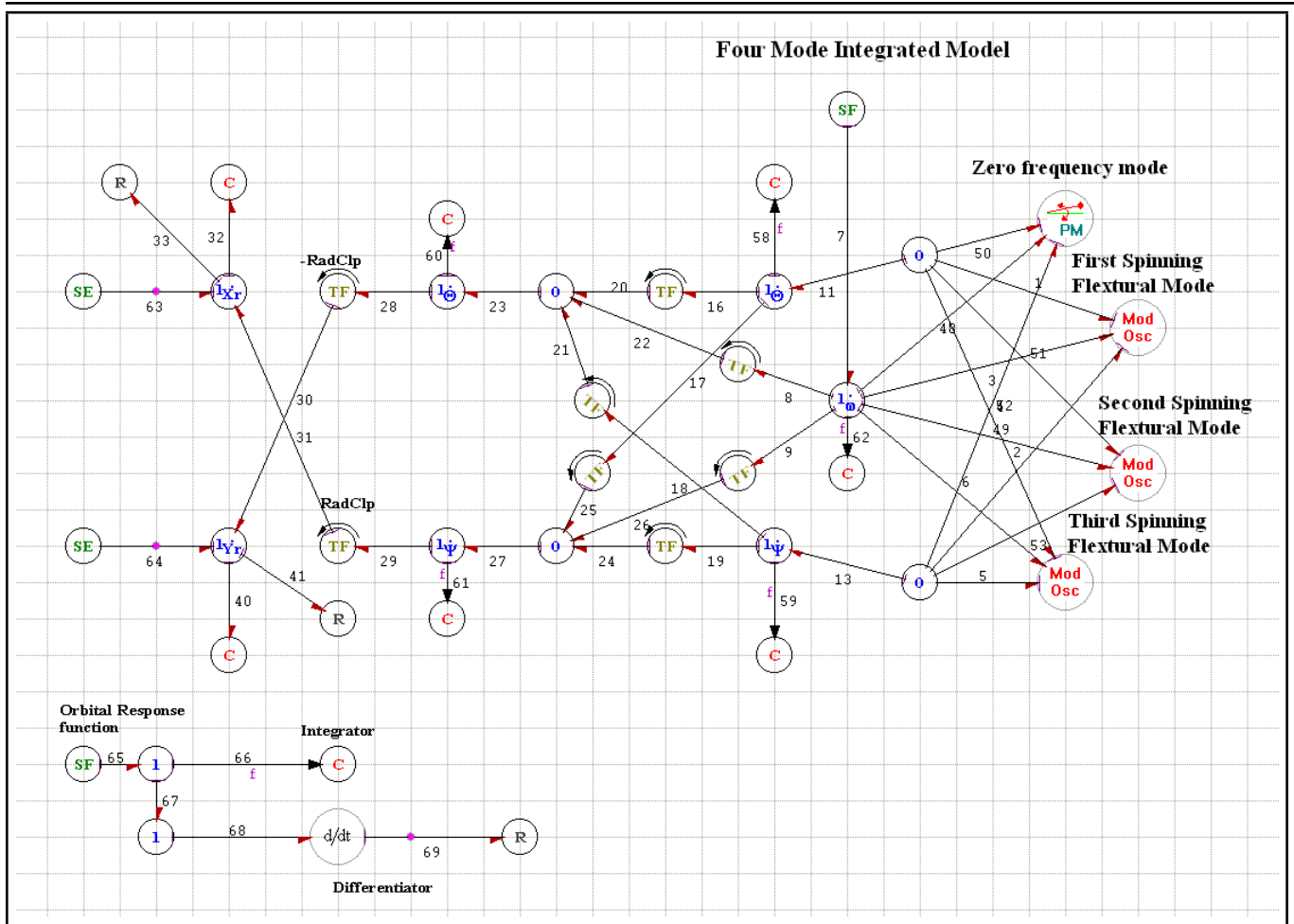


Figure 9. The integrated Bond graph model with three flexural modes.

Table 1. Simulation parameters for the rotor.

Parameter name	Tentative value	Remarks
ShaftAngSpeed	150	Shaft Angular Speed in Hz.
BeamLen	0.4	Length of the Rotor Shaft.
RadRotor	0.04	Radius of the Rotor Shaft.
Rho	7800.0	Density of Rotor Material.
E	2.1e+10	Young's Modulus of Rotor Material.
NuInt	0.0004	Internal Damping Parameter.
NuExt	0.0004	External Damping Parameter.
RadCp	0.08	Radius of Coupling
Rcpl	1.0e+5	Axial Damping of Coupling
Kcpl	1.0e+8	Axial Stiffness of Coupling
PM_Eps	0.000001	Equivalent unbalance of eccentricity PenMode
FLM1_FIMn	1	Flexural Mode Number (Integer >0)
FLM1_EpsMn	0.000001	Modal Eccentricity.
FLM2_FIMn	2	Flexural Mode Number (Integer >0)
FLM2_EpsMn	0.000001	Modal Eccentricity.
FLM3_FIMn	3	Flexural Mode Number (Integer >0)
FLM3_EpsMn	0.000001	Modal Eccentricity.
PM_RaPM	2.0	Pendulum Mode External Damping
SlcResF	1	SlcResF: Orbital Response Function = 1
Alf	0.0	Alf
Beta	0.0	Beta
Sigma	0.0	Sigma

Table 2. Controller tuning parameters.

Alfa	1.0E+4
Beta	1.0E+12
Sigma	10.0

of action by giving them zero values. Higher modal components that are the second and third modal components in static frame are stabilized with convergence of the whirling motion. It is easily seen that in spite of the non-potential nature of the circulating force which rendered instability in an uncontrolled rotor system, it is smoothly stabilized by the whirl orbital response control action.

9. CONCLUSION

The influence of shaft flexibility causing participation on flexural modes on the efficacy of the proposed stabilization strategy is studied. Rotors are assumed to be rotating at medium speeds, i.e., speeds which are high enough to render the pendulum or tool mode unstable when no active stabilization is in action. The ratification reported in the final phase of the work also creates ground for stabilization of very high-speed rotors. However, this study is confined to medium-speed (as defined above) rotors. We could also show how modal separation was possible using the normalized orthogonal operations and how the modal bond graph could be drawn using Symbols Sonata. For Low flexural modal oscillations, we

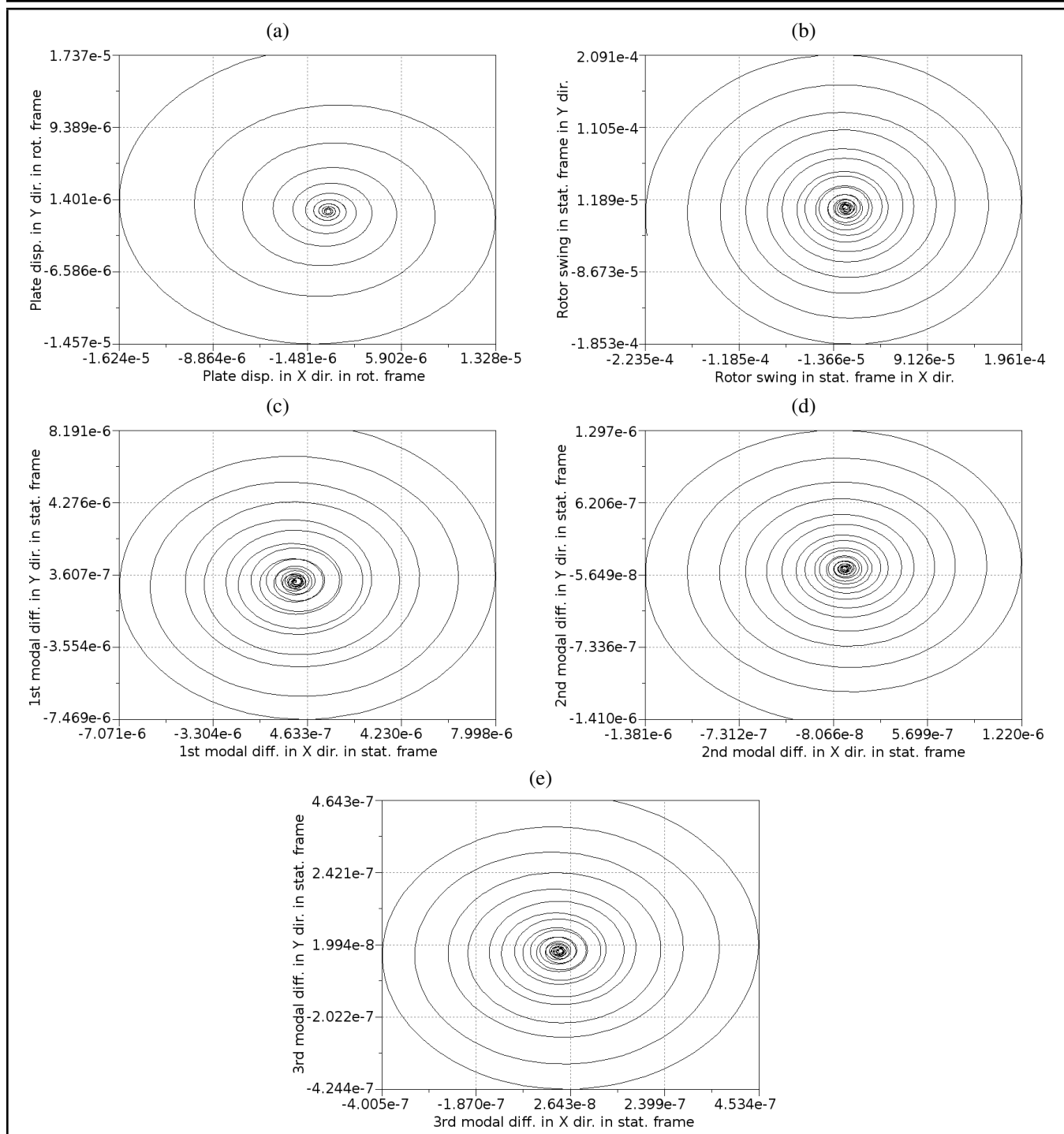


Figure 10. (a) Plate Displacement of Y direction in rotating frame. (b) Rotor swing of Y direction in static frame. (c) 1st modal deflection of Y direction in static frame. (d) 2nd modal deflection of Y direction in static frame. (e) 3rd modal deflection of Y direction in static frame.

could stabilize the system using the existing stabilizing strategy but we need to check the efficacy of this control strategy for higher modal frequencies in future work. Presently, we have taken a constant speed motor whose dynamics are relatively much stronger than the whirling shaft but in the future we need to extend the work on the effects of the whirling shaft on the dynamics of the motor and nature of imbalances which may occur in the motor side due to the rotating shaft.

REFERENCES

- 1 Crandall, S.H., Karnopp, D.C., and Kurtz, D.C. *Dynamics of mechanical and electromechanical systems*, McGraw-Hill, (1968).
- 2 Holmes, R. Nonlinear performance of squeeze film bearings, *J. of Mechanical Engineering Science*, **14** (1), 74-77, (1972). https://dx.doi.org/10.1243/JMES_JOUR_1972_014_011_02
- 3 Margolis, D.L. Bond graphs, normal modes and vehicular

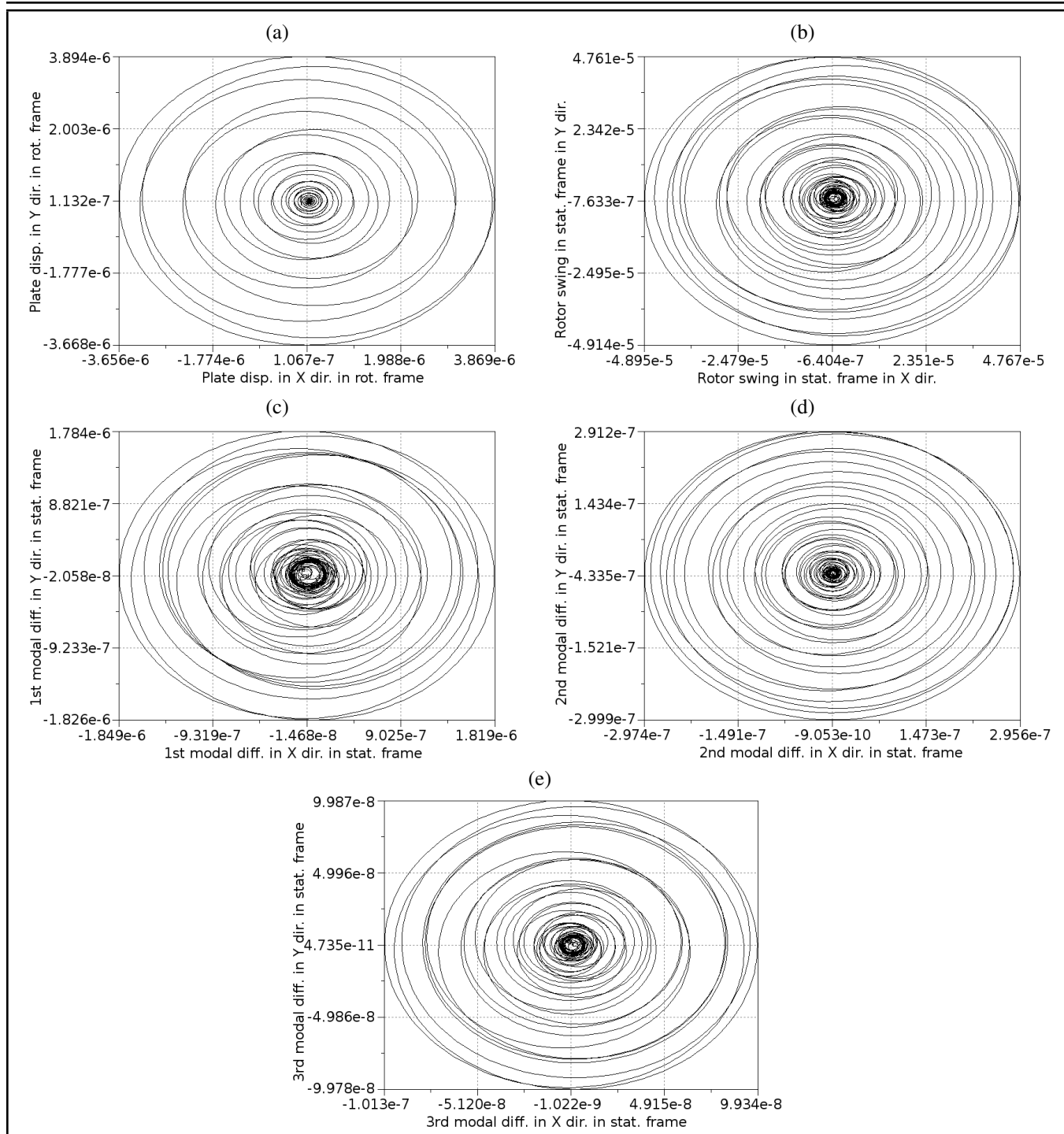


Figure 11. (a) Plate Displacement of Y direction in rotating frame. (b) Rotor swing of Y direction in static frame. (c) 1st modal deflection of Y direction in static frame. (d) 2nd modal deflection of Y direction in static frame. (e) 3rd modal deflection of Y direction in static frame.

structures, *Vehicle System Dynamics*, **7** (1), 49–63, (1978). <https://dx.doi.org/10.1080/00423117808968551>

⁴ Margolis, D.L. Bond graphs for distributed system models admitting mixed causal inputs, *J. Dyn. Sys., Meas., Control*, **102** (2), 94–100, (1980). <https://dx.doi.org/10.1115/1.3149602>

⁵ Margolis, D.L. Dynamical models for multidimensional structures using bond graphs, *J. Dyn. Sys., Meas., Control*, **102** (3), 180–187, (1980). <https://dx.doi.org/10.1115/1.3139631>

⁶ Rosenberg, R.C. and Karnopp, D. *Introduction to physical system dynamics*, McGraw-Hill, New York, (1983).

⁷ Margolis D. L., Karnopp, D. C., and Rosenberg, C. R. *System dynamics: a unified approach*, John Wiley and Sons, (1990).

⁸ Kirillov, O. N. Gyroscopic stabilization in the presence of non-conservative forces, *Dokl. Math.*, **76** (2), 780–785, (2007). <https://dx.doi.org/10.1134/S1064562407050353>

⁹ Glebov, V. V., Sorokin, V. M., Puchkov, V.P. and Ignat’ev, D. A. Eliminating vibrations in the face grinding of glass,

- Russian Engineering Research*, **27** (5), 305–308, (2007). <https://dx.doi.org/10.3103/s1068798x07050164>
- ¹⁰ Bou-Rabee, N.M., Marsden, J. E., and Romero, L. A. Dissipation-induced heteroclinic orbits in tippe tops, *SIAM Review*, **50** (2), 325–344, (2008). <https://dx.doi.org/10.1137/080716177>
- ¹¹ Margolis, D.L. A survey of bond graph modeling for interacting lumped and distributed systems, *J. Franklin Inst.*, **319** (1-2), 125–135, (1985). [https://dx.doi.org/10.1016/0016-0032\(85\)90069-9](https://dx.doi.org/10.1016/0016-0032(85)90069-9)
- ¹² Simo, J.C. and Vu-Quoc, L. On the dynamics of flexible beams under large overall motions the plane case: part ii, *J. Appl. Mech.*, **53** (4), 855–863, (1986). <https://dx.doi.org/10.1115/1.3171871>
- ¹³ Meirovitch, L. and Baruah, H. On the robustness of independent modal space control method. *Journal of Guidance, Control, and Dynamics*, **6** (1), 20–25, (1983). <https://dx.doi.org/10.2514/3.19797>
- ¹⁴ Book, W.J., and Majette, M. Controller design for flexible distributed parameter mechanical arm via combined state space and frequency domain techniques, *J. Dyn. Sys., Meas., Control*, **105** (4), 245–254 (1983). <https://dx.doi.org/10.1115/1.3140666>
- ¹⁵ Burke, S.E. and Hubbard, J.E., Jr. Active vibration control of simple supported beam using spatially distributed actuator, *IEEE Control System Mag.*, **7** (4), 25–30, (1987). <https://dx.doi.org/10.1109/MCS.1987.1105349>
- ¹⁶ Plump, J.M., Hubbard, J.E., Jr., and Bailey, T. Nonlinear control of a distributed system: simulation and experiment results, *J. Dyn. Sys., Meas., Control*, **109** (2), 133–139, (1987). <https://dx.doi.org/10.1115/1.3143830>
- ¹⁷ Baz, A. and Poh, S. Experimental implementation of modified modal space control method, *Journal of Sound and Vibration*, **139** (1), 133–149, (1990). [https://dx.doi.org/10.1016/0022-460X\(90\)90780-4](https://dx.doi.org/10.1016/0022-460X(90)90780-4)
- ¹⁸ Morris, K. and Vidyasagar, M. A comparison of different models for beam vibrations from standpoint of control design, *J. Dyn. Sys., Meas., Control*, **112** (3), 349–356, (1990). <https://dx.doi.org/10.1115/1.2896151>
- ¹⁹ Nathan, P.J. and Singh, S.N. Sliding mode control and elastic mode stabilization of a robotic arm with flexible links, *J. Dyn. Sys., Meas., Control*, **113** (4), 669–676, (1991). <https://dx.doi.org/10.1115/2896473>
- ²⁰ Tani, J., Chonan, S.S.K., Liu, Y., Takahashi, F., Ohtomo, K., and Fuda, Y. Digital active vibration control of a cantilever beam with piezo electric actuators, *JSME Int. Jour. Series 3*, **34** (2), 168–175, (1991). <https://dx.doi.org/10.1299/jsmec1988.34.168>
- ²¹ Tzou, H.S. Distributed modal identification and vibration control of continua: piezoelectric finite element formulation and analysis, *J. Dyn. Sys., Meas., Control*, **113** (3), 500–505, (1991). <https://dx.doi.org/10.1115/1.2896438>
- ²² Tzou, H.S., Tseng, C.I., and Wan, G.C. Distributed structural dynamics control of flexible manipulators. structural dynamics and distributed viscoelastic actuator, *Computers and Structures*, **35** (6), 669–677, (1990). [https://dx.doi.org/10.1016/0045-7949\(90\)90412-U](https://dx.doi.org/10.1016/0045-7949(90)90412-U)
- ²³ Smith, R.D. and Weldon, W.F. Nonlinear control of a rigid rotor magnetic bearing system: modeling and simulation with full state feedback, *IEEE Transaction on Magnetics*, **31** (2), (1995). <https://dx.doi.org/10.1109/20.364771>
- ²⁴ Vaz, J. A. C. *Theoretical and experimental studies on the dynamics and control of intelligent beam structure with special reference to flexible manipulators*, PhD Dissertation Department of Mechanical Engineering, Indian Institute of Technology, 1995 Kharagpur, Pin 721 302, India.
- ²⁵ Mukherjee A., and Sengupta, S. Active stabilization of rotors with circulating forces due to spinning dissipation, *Journal of Vibration and Control*, **17** (10), 1509–1524, (2011). doi10.1177/1077546310380728
- ²⁶ Mukherjee, A. and Sengupta, S. A proposal for active control of face abrasive tool wandering, *Journal of Vibration and Control*, **17** (14), 2175–2186, (2011). <https://dx.doi.org/10.1177/1077546311402708>
- ²⁷ Holmes, R., Nonlinear performance of squeeze film bearings, *J. of Mechanical Engineering Science*, **14** (1), pp. 74–77, (1972). https://dx.doi.org/10.1243/JMES_JOUR_1972_014_011_02
- ²⁸ Mukherjee A., Karmakar, R., and Samantaray, A.K. *Bond graph in modeling, simulation and fault identification*, I.K. International Pvt. Ltd., New Delhi, (2006).
- ²⁹ Baz A. and Poh S., Performance of an active Control System with Piezo electric actuators, *Journal of sound and Vibration*, **126**(2), p.327–324, (1988).
- ³⁰ Halder B., Mukherjee A., and Karmakar R., Theoretical and Experimental Studies on Squeeze Film Stabilizer for Flexible Rotor-Bearing Systems Using Newtonian and Viscoelastic Lubricants *Jr. of Vibration and Acoustics, Transaction of ASME*, **112**(4), 473–482, (1990).
- ³¹ Preumont A., Dufour J. and Malekian C., Active Damping by a Local force Feed Back with Piezo Actuators, *Journal of Guidance and control.*, **12**(2), pp. 390–395, (1992).
- ³² Active stabilization of rotors with circulating forces due to spinning dissipation *Journal of Vibration and Control* September 2011 17: 1509-1524, November 22, 2010
- ³³ A proposal for active control of face abrasive tool wandering *Journal of Vibration and Control*1077546311402708, first published on May 20, 2011